Materials Science in Semiconductor Processing 169 (2024) 107874

Contents lists available at ScienceDirect

Materials Science in Semiconductor Processing

journal homepage: www.elsevier.com/locate/mssp

Enhancing industrialization TOPCon solar cell efficiency via comprehensive anti-reflection passivation film optimization

Wenhao Chen [a,b,*], Shengxing Zhou [b], Weiqing Liu [b], Yingming Wang [b,**], Penghui Chen [c], Yuanyuan Yu [c], Yimao Wan [c]

[a] Key Laboratory of Nondestructive Testing (Nanchang Hangkong University), Ministry of Education, Nanchang, 330063, China
[b] School of Testing and Photoelectric Engineering, Nanchang Hangkong University, Nanchang, 330063, China
[c] Center of Cell Research, Risen Energy Co., Ltd., Ningbo, 315609, China

ARTICLE INFO

Keywords:
Silicon solar cell
TOPCon
Plasma oxidation
Plasma hydrogenation

ABSTRACT

This study focuses on enhancing the performance of n-type Tunnel Oxide Passivated Contact (TOPCon) solar cells by exploring the optimization of both front and rear film layers. For the front film, we implement a one-step plasma oxidation process before depositing silicon nitride on alumina, aiming to enhance the quality of the alumina layer and improve overall passivation. In the case of the rear film, we introduce a NH_3 plasma treatment to elevate hydrogen content of SiN_x. These additional hydrogens diffuse into the interfacial silicon oxide during the firing process to help reduce the number of surface dangling bonds and inhibit the degradation of the passivating contacts, which significantly contributes to enhanced passivation quality. Through separate optimization of these film layers, we aim to harness the full potential of TOPCon solar cells, achieving remarkable improvements in passivation quality and overall performance. With the help of XRD, SIMS, QSSPC, ellipsometry and other characterization tools, the underlying reasons for the improved passivation quality due to plasma oxidation and plasma hydrogenation were explored. Finally, plasma oxidation and hydrogenation lead to ~0.06 and ~0.07% average efficiency enhancements, respectively.

1. Introduction

In recent years, significant advancements have been made in solar cell technologies, with the introduction of Tunnel Oxide Passivated Contact (TOPCon) solar cells being one of the most noteworthy breakthroughs [1–5]. TOPCon solar cells have exhibited superior efficiency and passivation properties compared to traditional silicon solar cells, making them an attractive option for large-scale photovoltaic applications. The core of the TOPCon comprises an ultra-thin oxide layer and a heavily doped polycrystalline silicon layer, which enables selective carrier transport, resulting in a combination of outstanding passivation quality and contact performance [6–8]. Regrettably, the application of this passivating contact on the solar cell front side presents challenges due to its intense light parasitic absorption, primarily attributed to the heavily doped polysilicon layer [9]. Indeed, in the current TOPCon solar cell continues the design of traditional solar cells, the front structure employs a boron homogeneous/selectivity emitter in combination with passivation and anti-reflection film layers, such as alumina (AlO_x) and silicon nitride (SiN_x) [10,11]. Furthermore, the polysilicon passivating contact structure, when subjected to the firing process required for metallization, can suffer from substantial degradation in passivation quality [12]. To address this issue, a frequent practice is to shield the polysilicon with a hydrogen-rich SiN_x film, which effectively prevents the occurrence of passivation quality degradation and leads to a notable improvement in the overall passivation performance, due to the presence of hydrogen [13]. The significance of hydrogen content in the structural performance of doped polysilicon passivating contacts has been well-documented in extensive studies. It has been consistently shown that maintaining a higher concentration of hydrogen in the vicinity of the ultrathin oxide layer, achieved through various methods, can significantly enhance passivation quality [14–17]. And finally leading to a notable improvement in the electrical performance of TOPCon solar cells [18].

In this work, our primary objective was to optimize the front and rear

* Corresponding author. Key Laboratory of Nondestructive Testing (Nanchang Hangkong University), Ministry of Education, Nanchang 330063, China.
** Corresponding author.
E-mail addresses: whchen@nchu.edu.cn (W. Chen), wym@nchu.edu.cn (Y. Wang).

https://doi.org/10.1016/j.mssp.2023.107874
Received 14 August 2023; Received in revised form 10 September 2023; Accepted 29 September 2023
Available online 4 October 2023

stacked passivation films independently for TOPCon solar cells, with the aim of enhancing their overall passivation quality. The passivation film on the front side of the TOPCon solar cell consists of five distinct layers, arranged from bottom to top as follows: AlO_x, two layers of SiN_x with different refractive indices *n*, silicon nitride oxide (SiO_xN_y), and a silicon oxide (SiO_x). This specific combination of layers has been widely adopted by mainstream TOPCon solar cell manufacturers due to its dual benefits in optics and electricity. It effectively achieves excellent surface passivation, minimizing recombination losses, while also providing a notable anti-reflective effect. On this foundation, a one-step plasma oxidation process was implemented prior to depositing SiN_x on AlO_x. The purpose of this process was to eliminate oxygen vacancy defects within the AlO_x layer, thus improving its passivating properties. For the rear passivation, a combination of three layers of silicon nitride with different *n* is used to achieve both passivation and optical performance. As a further optimization, a NH_3 plasma treatment was introduced to increase the hydrogen content before each layer of SiN_x deposition. Through this separate optimization of the front and rear film layers, better passivation quality can be observed without affecting the optical properties and the contact of the metal electrode with the silicon substrate. Finally, open-circuit voltage (V_{oc}) enhancement due to improved passivation quality aids further optimization of TOPCon solar cell conversion efficiency.

2. Experimentals

The silicon wafers employed for the fabrication of TOPCon solar cells are of industrial grade, with a size of 182 mm × 182 mm in square and a thickness of ~150 μm, the structure of the adopted TOPCon solar cell is schematically shown in Fig. 1. These n-type substrates boast a resistivity range of 0.5–2 Ω cm. Subjecting all wafers to a sequence of standard cleaning and texturing etching procedures. Following by a series of critical processes to established selective boron emitters on the front side of the wafers: thermal boron diffusion, laser treatment, and post thermal oxidation, ensuring controlled sheet resistances of ~250 Ω/□ in the light doped region and ~90 Ω/□ in the heavy doped region. Following this step, the borosilicate glass layer was removed from the rear and edge of the wafer, leaving the front surface intact. Subsequently, the wafer underwent an alkali polishing process to remove the boron emitter on the rear and edge. On the polished surface, an ultra-thin tunneling oxide layer, ~1.5 nm, was generated through oxidation with O_2 plasma. This was followed by the deposition of an in-situ phosphorus-doped amorphous silicon layer, ~115 nm thick, using an in-line magnetron sputtering system (JT8000 POPAID, Belightech). Phosphorus-doped silicon targets are used for phosphorus-doped a-Si deposition, and the plasma excited from Ar and PH_3 precursor gases is introduced to increase phosphorus content, and the gas flow rate of Ar and PH_3 can be independently controlled by three successively distributed zones. After

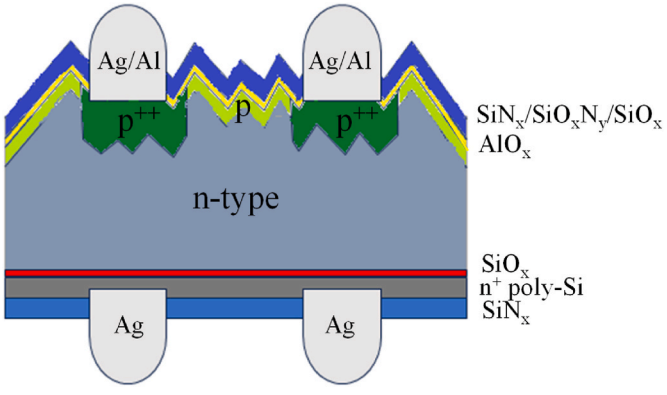

Fig. 1. Schematic diagram of the adopted commercial TOPCon solar cell structure.

860 °C, 30 min thermal annealing at dry N_2 environment, single-sided polysilicon passivating contact structure was formed on the rear [19].

After removing the borosilicate glass and phosphor-silicate glass from the surface of the wafer, the preparation of the anti-reflection passivation film on the front side starts with the deposition of a ~10 nm AlO_x film by an in-line single side deposition atomic layer deposition (ALD) (Ideal Deposition Equipment & Applications Co., Ltd.), which is the most mainstream commercial TOPCon solar cell AlOx deposition equipment available. Subsequently, SiN_x, SiO_xN_y and SiO_x were sequentially deposited on AlO_x with a tubular PECVD equipment (M82300-12/UM, Red Solar Photoelectric Technology Co., Ltd.), and in order to further enhance the film formation quality of AlO_x, a N_2O plasma treatment (plasma oxidation, PO) was set up for 120 s prior to the start of the process, and the specific process setup is shown in Table 1. The process involves heating precursor gases, which is then excited by pulsed radio frequency to create a glow discharge, forming a plasma. Two corresponding graphite sheets are subjected to opposite alternating voltage, which accelerates the plasma to impact the gas between the plates. This action propels the plasma towards the surface of the silicon wafer, thereby completing the coating process. For the rear side, three layers of SiN_x with different refractive indices were deposited sequentially using a same type tubular PECVD, while plasma hydrogenation (PH) using NH_3 as a precursor gas was performed prior to the deposition of each SiN_x, and the main processes are also listed in Table 1. Finally, the fabrication of TOPCon solar cells is completed by going through the standard screen printing and firing process.

The *I–V* characteristics of the TOPCon solar cells are assessed using a solar simulator that replicates sunlight conditions. Quantum efficiency (QE, Enlitech) tester is used to assist in analyzing TOPCon solar cell performance. The evaluation of passivation quality for both the front and rear passivation film layers, both post-deposition and after the firing process, is conducted using implied open circuit voltage (iV_{oc}). This parameter is obtained using Quasisteady-state photoconductance (QSSPC) measurements performed under 1-Sun equivalent light intensity with a Sinton WCT-120 lifetime tester [20]. An ellipsometry (EMPro-PV, ELLITOP) is used to monitor the refractive index and thickness variations of the deposited film. X-ray Photoelectron Spectroscopy (XPS) (Axis Ultra DLD, KRATOS) equipped with an Al Kα monochromatic X-ray source ($h\nu = 1486.6$ eV) was utilized to compare the impact of plasma oxidation on the deposited AlO_x layers. Additionally, in order to evaluate the impact of plasma hydrogenation on the hydrogen content within the SiN_x layers, we utilized Time-of-Flight Secondary Ion Mass Spectrometry (TOF-SIMS 5 iontof, PHI Nano-TOFII). This analysis employed a Cs + primary ion at 10 kV, with the sample set at a −5 kV potential to detect negative secondary ions. The analysis was performed with an impact energy of 15 kV.

3. Results and discussion

3.1. Plasma oxidation

The impact of the PO treatment on the properties of the AlO_x film is visually illustrated through the O 1s core level spectra within the X-ray Photoelectron Spectroscopy (XPS) results, as displayed in Fig. 2a. Prior to the peak fitting process, the Shirley background, accounting for inelastically scattered electrons, was eliminated. From the O 1s peak, peaks at ~530.8 eV and ~532.9 eV were meticulously deconvoluted. These correspond to the O–Al–O bands of Al_2O_3 and Al–OH bands of $Al(OH)_3$, respectively. We used the peak areas of the O–Al–O and Al–OH contributions within the O1s core levels to analysis the ratio changes of Al_2O_3 to $Al(OH)_3$. The band ratio is only 1.22 in AlO_x films that have undergone only the same thermal process without plasma treatment, whereas the application of plasma oxidation increases the ratio to 1.66 [21,22]. It stems from the design of our industrial in-line ALD system, which effectively balances capacity and cost considerations. In the system, the sample is conveyed on a transfer plate through the

Table 1
PO and PH process setting table for the front and rear film deposition process.

	Step	Time (s)	NH_3 flow (sccm)	SiH_4 flow (sccm)	N_2O flow (sccm)	Power (W)	Pressure (mbar)
Front	Plasma oxidation	120	0	0	12,000	14,000	1650
	SiN_x deposition	100	9335	2800	0	14,000	1650
		260	10,665	2000	0	15,500	1650
		180	10,655	1400	0	16,500	1650
	SiO_xN_y deposition	124	5200	1200	7400	14,400	1000
		144	5200	900	8935	14,400	1000
	SiO_x deposition	96	0	900	11,735	14,400	900
Rear	Plasma hydrogenation	50	12,000	0	0	15,000	1800
	SiN_x deposition	145	9800	2200	0	15,500	1800
	Plasma hydrogenation	50	16,000	0	0	15,500	1900
	SiN_x deposition	180	14,000	2000	0	16,500	1900
	Plasma hydrogenation	50	15,200	0	0	15,500	1900
	SiN_x deposition	390	14,400	1400	0	16,500	1900

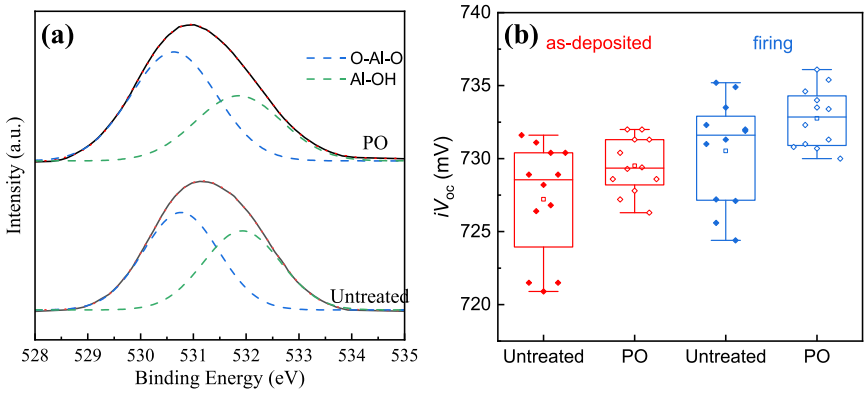

Fig. 2. The change of AlOx XPS results at O 1s peak caused by PO treatment (a) and the effect on iV_{oc} values of final sample (b).

trimethylaluminum (TMA) and H_2O chambers, undergoing recirculation until the desired thickness is achieved. However, the absence of stringent demarcation between the TMA and H_2O regions gives rise to a less than optimal quality in the deposited AlO_x film. It tends to harbor a significant quantity of oxygen vacancy defects and Al–OH bonds that fail to break in time, which remain intertwined due to their overlapping deposition processes. The integration of the PO process resulted in an elevation of the O–Al–O bond ratio, which can be attributed to the vigorous high-energy plasma bombardment, causing the rupture of O–H bonds. Consequently, the released Al and O from plasma reconfigure to form additional O–Al–O bonds, that aids in mitigating oxygen vacancy defects. Simultaneously, the liberated hydrogen from the fractured O–H bonds permeates into both the AlO_x film and the AlO_x/Si interface [23]. The collective impact plays a pivotal role in diminishing the density of defect states on the Si wafer surface. As a result, the effect of PO process on the values of the pre-metallization samples as shown in Fig. 2b. The PO process effectively improved the iV_{oc} values, and the average iV_{oc} values increased by more than 2 mV compared to untreated samples, both as-deposited and after firing, while at the same time the dispersion of the data distributions was much smaller, indicating that the homogeneity of the passivation had been significantly improved.

The final average electrical performance comparisons of TOPCon solar cells are shown in Table 2. The addition of extra PO treatment to the deposition process of the front surface passivation film helps the TOPCon solar cell to obtain an average V_{oc} gain of 1.3 mV. In addition, the fill factor (*FF*) is also obtaining a slight rise. There are two possible reasons for this, one is the higher V_{oc} due to better surface passivation quality which helps to increase the *FF*, and the other is that the PO treated AlO_x film may be more easily penetrated by the metal paste to obtain lower contact resistivity. The overall effect on the cell conversion efficiency is an absolute average efficiency gain of 0.06%. The comparative analysis of QE and reflectance in Fig. 3 reveals that the PO treatment induces a marginal increase in reflectance within the 300–400 nm wavelength range. This change can be attributed to the slight alteration in the optical properties of the AlO_x films resulting from the PO treatment. Specifically, the refractive index *n* of AlO_x demonstrates a decrease from 1.63 to 1.60 by PO, as measured by ellipsometry. However, no significant effect on the AlO_x thickness is observed following the PO treatment. Furthermore, the PO treatment has a

Table 2
Effect of PO treatment on electrical performance of TOPCon solar cells.

	Quantity	V_{oc} (mV)	I_{sc} (A)	*FF* (%)	Eta (%)
Untreated	1931	721.5	13.69	84.07	25.07
PO	1845	722.8	13.69	84.11	25.13

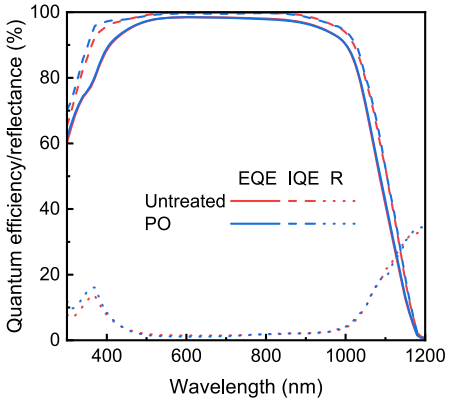

Fig. 3. Effect of PO treatment on the quantum efficiency of TOPCon solar cells.

notably positive impact on the internal quantum efficiency (IQE) performance within the 300–400 nm wavelength range, due to the improved quality of the front surface passivation as shown in Fig. 2b. Nonetheless, the gain in external quantum efficiency (EQE) is not as apparent due to optical losses, which underscores the primary reason that the electrical performance enhancement resulting from the PO process primarily manifests in the V_{oc} gain, while any changes in I_{sc} are not readily discernible.

3.2. Plasma hydrogenation

The impact of PH treatment on the distribution of H atoms within both the SiN_x layer and the polysilicon passivating contact structure is elucidated through SIMS analysis, as showcased in Fig. 4a. Following the completion of SiN_x deposition, the PH treatment leads to a notable increase in H content within the deposited SiN_x layer can be measured, escalating from ~6×10^{21} to ~1×10^{22} cm^{-3}. However, it exerts a lesser influence on the H content within the polysilicon layer as well as the tunneling oxide layer. Consequently, at this stage, PH treatment does not result in a significant change in passivation quality, as demonstrated in Fig. 4b. Upon subjecting the samples to the firing process, an essential step in the metallization of TOPCon solar cells, H atoms commence diffusion within the polysilicon passivating contacts and the underlying silicon substrate [24]. Notably, these H atoms accumulate near the interface SiO_x, consistent with findings reported in the literature [25]. In samples that underwent the PH process, the H content within the polysilicon and silicon substrate, particularly in the vicinity of SiO_x, is significantly higher compared to samples without PH treatment. This enrichment of H atoms near SiO_x proves beneficial as it contributes to a reduction in the density of unsaturated suspended bonds on the silicon surface. Moreover, the higher H content more effectively inhibits the passivation quality degradation of the passivating contacts during the firing process [13,26]. The outcome is evident in the samples subjected to PH treatment, displaying higher mean values of iV_{oc} (~2.1 mV higher than samples without PH treatment), accompanied by a reduction in the dispersion of iV_{oc} values, as shown in Fig. 4b. This clear trend underscores the pronounced effect of PH introduction in enhancing passivation quality.

In addition to enhancing passivation quality, PH treatment proves beneficial in elevating the overall electrical performance of TOPCon solar cells, as evidenced by the results presented in Table 3. The improvement in passivation quality contributes to a notable V_{oc} enhancement of approximately 1.1 mV. Importantly, there are no significant differences observed in the performance of I_{sc} and *FF*. This outcome aligns with the observation that PH treatment exerts minimal influence on the thickness and refractive index of the final SiN_x film, as determined by ellipsometry analysis. Finally, TOPCon solar cells achieve ~0.07% average conversion efficiency gain by PH processing.

Table 3
Effect of PH treatment on electrical performance of TOPCon solar cells.

	Quantity	V_{oc} (mV)	I_{sc} (A)	*FF* (%)	Eta (%)
Untreated	4368	722.8	13.66	84.04	25.05
PH	4889	723.9	13.68	84.02	25.12

4. Conclusions

In conclusion, our study has highlighted significant achievements in the optimization of TOPCon solar cells, with two key approaches on the anti-reflection passivation films. Firstly, for the front side film, we implemented a one-step PO process utilizing N_2O plasma. This process remarkably enhanced the quality of the in-line ALD-deposited AlOx film by repairing the oxygen vacancy defects within it. The disruption of O–H bonds during this process additionally released H, contributing to passivation quality enhancement, evident by an impressive ~2 mV increases in iV_{oc}, which ultimately resulted in a 0.06% improvement in efficiency. Furthermore, the application of the PH process prior to the deposition of each SiN_x layer on the rear side of the cell demonstrated compelling results. The SIMS analysis showed a significant increase in H content within SiN_x post-deposition. After the firing process, these H atoms diffuse towards the passivating contact and silicon substrate, becoming enriched in the SiO_x region. This enrichment effectively reduces the number of surface dangling bonds and helps inhibit the degradation of the passivating contact during firing. Consequently, the iV_{oc} value of the PH-treated sample demonstrated a substantial ~2.1 mV increase compared to the untreated sample post-firing. This enhancement in the final electrical performance translated to an average efficiency gain of ~0.07% for the TOPCon solar cells. The observed improvements in passivation quality and electrical performance demonstrate the potential of these optimization strategies in advancing TOPCon solar cell technology.

CRediT authorship contribution statement

Wenhao Chen: Conceptualization. **Shengxing Zhou:** Investigation, Validation. **Weiqing Liu:** Investigation. **Yingming Wang:** Resources, Writing – review & editing. **Penghui Chen:** Investigation. **Yuanyuan Yu:** Investigation. **Yimao Wan:** Resources.

Declaration of competing interest

The authors declare that they have no known competing financial interests or personal relationships that could have appeared to influence the work reported in this paper.

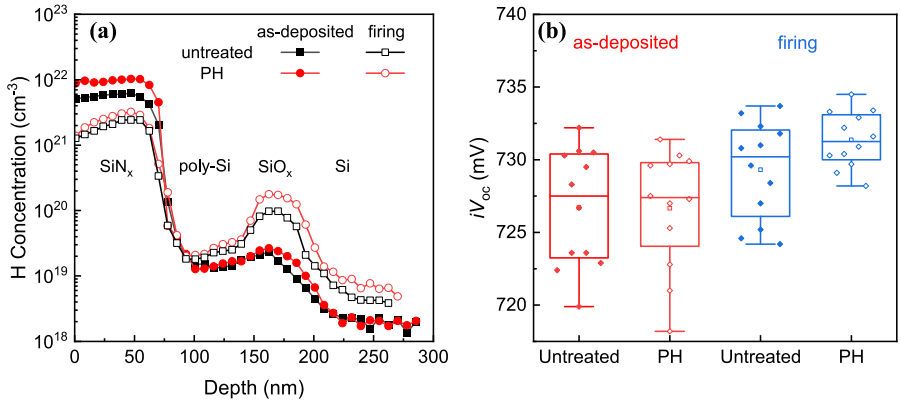

Fig. 4. Changes in H atom distribution caused by PH processing by SIMS extraction (a) and the effect on iV_{oc} values of final sample (b).

Data availability

Data will be made available on request.

Acknowledgment

This work has been supported by the National Natural Science Foundation of China (62204106), the Shangrao Technology Project (No. 2022A004) and the Key R&D Projects of Jiangxi Province (No. 20223BBE51026, No. 20232BBE50035).

References

[1] D.K. Ghosh, S. Bose, G. Das, S. Acharyya, A. Nandi, S. Mukhopadhyay, A. Sengupta, Fundamentals, present status and future perspective of TOPCon solar cells: a comprehensive review, Surface. Interfac. 30 (2022), 101917.
[2] B. Kafle, B.S. Goraya, S. Mack, F. Feldmann, S. Nold, J. Rentsch, TOPCon–technology options for cost efficient industrial manufacturing, Sol. Energy Mater. Sol. Cell. 227 (2021), 111100.
[3] T.G. Allen, J. Bullock, X. Yang, A. Javey, S. De Wolf, Passivating contacts for crystalline silicon solar cells, Nat. Energy 4 (11) (2019) 914–928.
[4] S.W. Glunz, B. Steinhauser, J.I. Polzin, C. Luderer, B. Grübel, T. Niewelt, A. M. Okasha, M. Bories, H. Nagel, K. Krieg, Silicon-based passivating contacts: the TOPCon route, Prog. Photovoltaics Res. Appl. 31 (4) (2023) 341–359.
[5] S.P. Muduli, P. Kale, State-of-the-art passivation strategies of c-Si for photovoltaic applications: a review, Mater. Sci. Semicond. Process. 154 (2023), 107202.
[6] F. Feldmann, G. Nogay, J.-I. Polzin, B. Steinhauser, A. Richter, A. Fell, C. Schmiga, M. Hermle, S.W. Glunz, A study on the charge carrier transport of passivating contacts, IEEE J. Photovoltaics 8 (6) (2018) 1503–1509.
[7] W. Liu, X. Yang, J. Kang, S. Li, L. Xu, S. Zhang, H. Xu, J. Peng, F. Xie, J.-H. Fu, Polysilicon passivating contacts for silicon solar cells: interface passivation and carrier transport mechanism, ACS Appl. Energy Mater. 2 (7) (2019) 4609–4617.
[8] F. Feldmann, G. Nogay, P. Löper, D.L. Young, B.G. Lee, P. Stradins, M. Hermle, S. W. Glunz, Charge carrier transport mechanisms of passivating contacts studied by temperature-dependent JV measurements, Sol. Energy Mater. Sol. Cell. 178 (2018) 15–19.
[9] F. Feldmann, M. Nicolai, R. Müller, C. Reichel, M. Hermle, Optical and electrical characterization of poly-Si/SiOx contacts and their implications on solar cell design, Energy Proc. 124 (2017) 31–37.
[10] D. Chen, Y. Chen, Z. Wang, J. Gong, C. Liu, Y. Zou, Y. He, Y. Wang, L. Yuan, W. Lin, 24.58% total area efficiency of screen-printed, large area industrial silicon solar cells with the tunnel oxide passivated contacts (i-TOPCon) design, Sol. Energy Mater. Sol. Cell. 206 (2020), 110258.
[11] Q. Wang, W. Wu, Y. Li, L. Yuan, S. Yang, Y. Sun, S. Yang, Q. Zhang, Y. Cao, H. Qu, Impact of boron doping on electrical performance and efficiency of n-TOPCon solar cell, Sol. Energy 227 (2021) 273–291.
[12] D. Kang, H.C. Sio, D. Yan, J. Stuckelberger, X. Zhang, D. Macdonald, Firing stability of phosphorus-doped polysilicon passivating contacts: factors affecting the degradation behavior, Sol. Energy Mater. Sol. Cell. 234 (2022), 111407.
[13] D. Kang, H.C. Sio, J. Stuckelberger, R. Liu, D. Yan, X. Zhang, D. Macdonald, Optimum hydrogen injection in phosphorus-doped polysilicon passivating contacts, ACS Appl. Mater. Interfaces 13 (46) (2021) 55164–55171.
[14] J.-I. Polzin, B. Hammann, T. Niewelt, W. Kwapil, M. Hermle, F. Feldmann, Thermal activation of hydrogen for defect passivation in poly-Si based passivating contacts, Sol. Energy Mater. Sol. Cell. 230 (2021), 111267.
[15] Y. Yang, P.P. Altermatt, Y. Cui, Y. Hu, D. Chen, L. Chen, G. Xu, X. Zhang, Y. Chen, P. Hamer, Effect of Carrier-Induced Hydrogenation on the Passivation of the poly-Si/SiOx/c-Si Interface, AIP Conference Proceedings, AIP Publishing, 2018.
[16] B.W. van de Loo, B. Macco, M. Schnabel, M.K. Stodolny, A.A. Mewe, D.L. Young, W. Nemeth, P. Stradins, W.M. Kessels, On the hydrogenation of Poly-Si passivating contacts by Al2O3 and SiNx thin films, Sol. Energy Mater. Sol. Cell. 215 (2020), 110592.
[17] M. Schnabel, B.W. Van De Loo, W. Nemeth, B. Macco, P. Stradins, W. Kessels, D. L. Young, Hydrogen passivation of poly-Si/SiOx contacts for Si solar cells using Al2O3 studied with deuterium, Appl. Phys. Lett. 112 (20) (2018).
[18] R. Chen, M. Wright, D. Chen, J. Yang, P. Zheng, X. Zhang, S. Wenham, A. Ciesla, 24.58% efficient commercial n-type silicon solar cells with hydrogenation, Prog. Photovoltaics Res. Appl. 29 (11) (2021) 1213–1218.
[19] W. Chen, X. Liu, W. Liu, Y. Yu, W. Wang, Y. Wan, Optimization of activated phosphorus concentration in recrystallized polysilicon layers for the n-TOPCon solar cell application, Sol. Energy Mater. Sol. Cell. 252 (2023), 112206.
[20] R.A. Sinton, A. Cuevas, M. Stuckings, Quasi-steady-state Photoconductance, a New Method for Solar Cell Material and Device Characterization, Conference Record of the Twenty Fifth IEEE Photovoltaic Specialists Conference-1996, IEEE, 1996, pp. 457–460.
[21] J. Haeberle, K. Henkel, H. Gargouri, F. Naumann, B. Gruska, M. Arens, M. Tallarida, D. Schmeißer, Ellipsometry and XPS comparative studies of thermal and plasma enhanced atomic layer deposited Al2O3-films, Beilstein J. Nanotechnol. 4 (1) (2013) 732–742.
[22] V. Naumann, M. Otto, R. Wehrspohn, M. Werner, C. Hagendorf, Interface and material characterization of thin ALD-Al2O3 layers on crystalline silicon, Energy Proc. 27 (2012) 312–318.
[23] L.Q. Zhu, Y.H. Liu, H.L. Zhang, H. Xiao, L.Q. Guo, Atomic layer deposited Al2O3 films for anti-reflectance and surface passivation applications, Appl. Surf. Sci. 288 (2014) 430–434.
[24] T.N. Truong, D. Yan, W. Chen, M. Tebyetekerwa, M. Young, M. Al-Jassim, A. Cuevas, D. Macdonald, H.T. Nguyen, Hydrogenation mechanisms of poly-Si/SiOx passivating contacts by different capping layers, Sol. RRL 4 (3) (2020), 1900476.
[25] M. Lehmann, N. Valle, J. Horzel, A. Pshenova, P. Wyss, M. Döbeli, M. Despeisse, S. Eswara, T. Wirtz, Q. Jeangros, Analysis of hydrogen distribution and migration in fired passivating contacts (FPC), Sol. Energy Mater. Sol. Cell. 200 (2019), 110018.
[26] Y. Shi, M.E. Jones, M.S. Meier, M. Wright, J.-I. Polzin, W. Kwapil, C. Fischer, M. C. Schubert, C. Grovenor, M. Moody, Towards accurate atom scale characterisation of hydrogen passivation of interfaces in TOPCon architectures, Sol. Energy Mater. Sol. Cell. 246 (2022), 111915.